

# HIGH-ALTITUDE DUST IN THE MARTIAN ATMOSPHERE

**Stephen R. Lewis, Liam J. Steele,** *Department of Physical Sciences, The Open University, Walton Hall, Milton Keynes MK7 6AA, UK (stephen.lewis@open.ac.uk)*, **François Forget,** *Laboratoire de Météorologie Dynamique (LMD), CNRS, IPSL, Paris, France.*

## Introduction:

We have conducted a study to assess the altitude to which a range of dust particle sizes might be transported under typical and dust storm conditions in the martian atmosphere. One aim has been to assess whether airborne dust particles originating from the lower atmosphere may interact with a spacecraft performing aerobraking maneuvers, and, if so, to evaluate the amount and nature of the dust particles. Such interactions may be problematic for spacecraft operations, but in the context of planetary protection issues (especially in the context of possible future sample return missions). The study also informs the design of prescribed dust scenarios for global climate modeling when it is undesirable to transport a full spectrum of dust particles interactively.

## Modelling studies:

Numerous modelling studies have been performed over the past two decades to try to understand the processes involved in the formation of martian dust storms, and dust transport in general (e.g. Basu et al. 2004, 2006; Forget 2008a,b; Kahre et al. 2006, 2008; Mulholland et al. 2013; Murphy et al. 1995; Newman et al. 2002a,b). The general consensus among these studies is that lifting by wind stress is responsible for the formation of dust storms in southern spring and summer, with dust devil lifting maintaining a background dust field during northern spring and summer. However, the spatial and temporal distribution of dust is still not accurately represented using interactive lifting. Few of these (Forget 2008a,b; Kahre et al. 2008) have specifically investigated particle size distributions or the height attained by the dust.

For the present study, we employ the most recent UK version of the LMD Mars global circulation model (MGCM) which is currently in use at the Open University and the University of Oxford. This MGCM uses the physical parameterizations shared with the LMD MGCM coupled to a UK-specific spectral dynamical core and semi-lagrangian advection scheme. It has been developed in a collaboration of the Laboratoire de Météorologie Dynamique, the Open University, the University of Oxford and the Instituto de Astrofísica de Andalucía (Forget et al. 1999). The model has been run with 32 unevenly-spaced vertical levels, stretched from the surface to about 130 km altitude.

Dust particles are discretized into 17 size bins ranging from 0.025–40  $\mu\text{m}$ , each with its own ex-

tinction coefficient  $Q_{\text{ext}}$ , appropriate for a wavelength of 670 nm. The lower limit is set at 0.025  $\mu\text{m}$  as dust particles smaller than about 0.02  $\mu\text{m}$  have negligible extinction (Forget 2008a). The dust is treated as fully radiatively active in the MGCM.

As we are interested in studying the vertical distribution of dust particles, and not specifically the methods of dust lifting, we use a simplified lifting scheme. In this scheme, dust particles are injected into the lowest model level of the atmosphere (centred about 4–5 m above the surface) with equal fluxes at all time-steps and at all grid-points that are free of CO<sub>2</sub> ice cover. The dust particle mass mixing ratios are scaled proportional to the mass distribution (i.e. proportional to  $r^3 n(r)$ ) to account for coagulation. Column optical depths are calculated by summing the dust opacity at each model level over the dust size bins and then summing the opacities over all the model levels. Modelled optical depths are then compared to observed optical depths obtained by binning and kriging TES retrievals (Montabone et al. 2014) and the dust mixing ratio in each bin is rescaled to match the model optical depth to the observation.

Turbulent mixing of dust is modelled in the atmospheric boundary layer by a 2.5-level Mellor-Yamada turbulence closure scheme, and dust is also mixed throughout the atmosphere by a dry convective adjustment scheme and a new thermals parametrization. The semi-lagrangian transport scheme advects each dust size bin according the large-scale winds predicted by the MGCM. Sedimentation rates for each dust size are calculated, including a Cunningham slip correction factor for the low martian atmospheric density. For the present study, particle agglomeration and scavenging by volatile condensation in the middle and lower atmosphere are not included; both would tend to preferentially deplete the smaller dust size bins, which can therefore be treated as upper estimates.

In order to set up the experiment in an unambiguous manner, the model was initialised by running a simulation of Mars Year 24 (MY24), but with the radiation scheme uncoupled and based on a prescribed vertical dust distribution rather than the multi-size dust bins which are transported by the model (which is initially injected very near the surface). At the end of MY24, the radiation scheme was coupled to the active dust distribution transported by the model and this run was continued throughout MY25 (labelled ‘Global dust storm’ since that year included the 2001 planet-encircling dust event) and

MY26 (labelled ‘No dust storm’ in the figures, since the year featured regional but not planet-encircling dust events), see Fig. 1. A final extreme case (labelled ‘Low dust density’) , was tested by repeating MY25 with the density of the dust particles reduced to a minimum value of  $1550 \text{ kg m}^{-3}$ , which corresponds to a composition of 98% zeolite and 2% magnetite with 30% porosity. In contrast, the standard density value used in the other experiments was  $2500 \text{ kg m}^{-3}$ , which corresponds to 95% feldspar and 5% magnetite with 10% porosity.

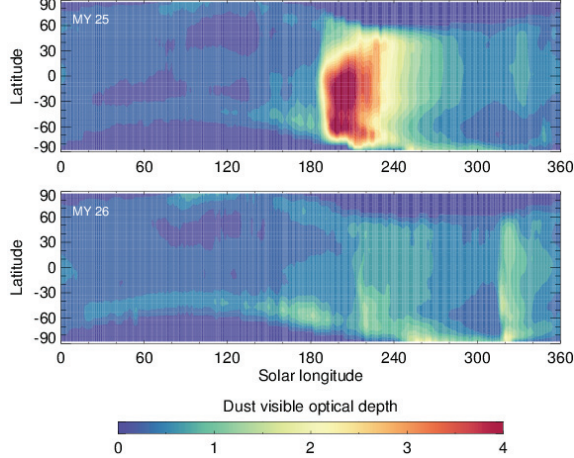


**Figure 1:** Zonally averaged visible dust optical depth for a year with a global dust storm (upper panel) and a year with only regional dust storms (lower panel).

Figure 2 illustrates the zonally averaged height of the ‘dust top’ for each of these three annual scenarios. The dust top is defined as the height where the dust mass mixing ratio falls below  $10^{-8} \text{ kg/kg}$ . Figure 3 shows the mass mixing ratio of zonally-averaged dust in a log-pressure versus latitude domain averaged over four cardinal ‘martian months’ for each scenario. Mixing ratios are averaged zonally and over  $30^\circ$  of areocentric longitude,  $L_S$ . Figure 4 instead shows the zonally-averaged effective dust radius in a log-pressure versus areocentric longitude domain at the equator. Both illustrate that dust is transported higher in the atmosphere at dustier times of year and that polar levels are generally depressed compared to equatorial dust.

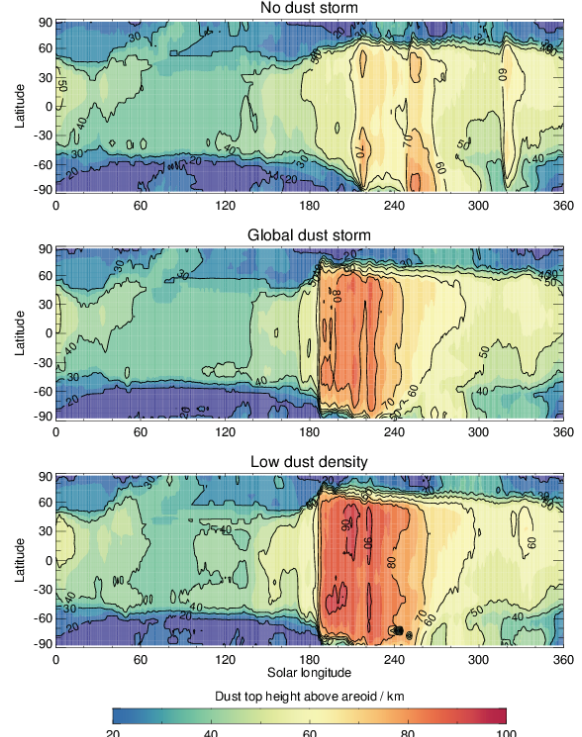


**Figure 2:** Zonally averaged height of the ‘dust top’ above the reference areoid.

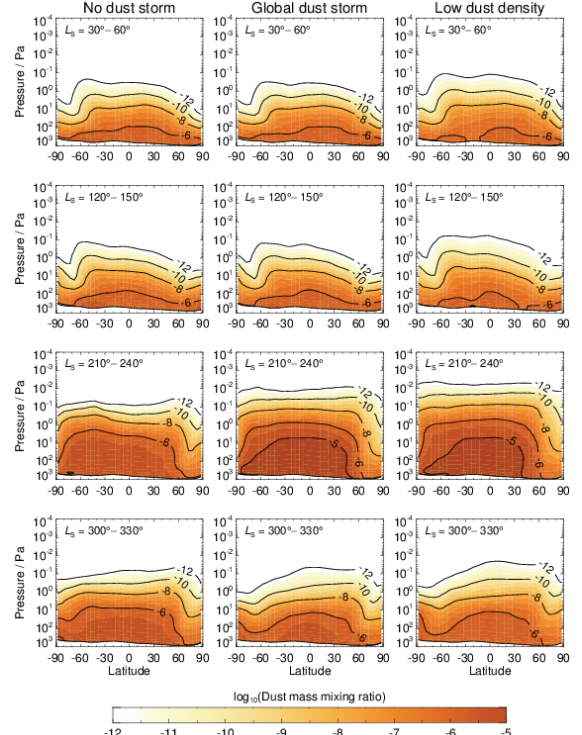


**Figure 3:** Dust mass mixing ratio at cardinal Mars months.

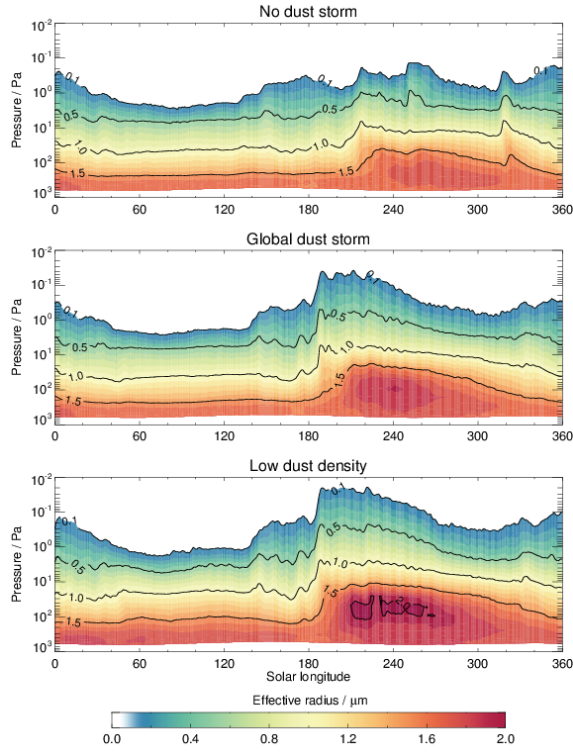


**Figure 4:** Dust effective radius zonally averaged at the equator.

It is notable that dust varies less strongly at a fixed pressure than it does at a fixed geometric height above the reference areoid. This is illustrated for one case in Figure 5, which shows the variation of the dust mass mixing ratio with season for a location on the equator and prime meridian in the MY25 simulation. The two lines represent the mixing ratio at constant height (100 km) and constant pressure (about  $10^{-3}$  Pa), chosen so that these are equivalent at  $L_S = 60^\circ$ . At the dustiest time of year ( $L_S = 190^\circ$ – $300^\circ$ ) the warming of the lower atmosphere causes expansion, raising the pressure at a fixed geometric height and so elevating the dust mixing ratio at a fixed geometric height by more than the dust mixing ratio changes at a fixed pressure.

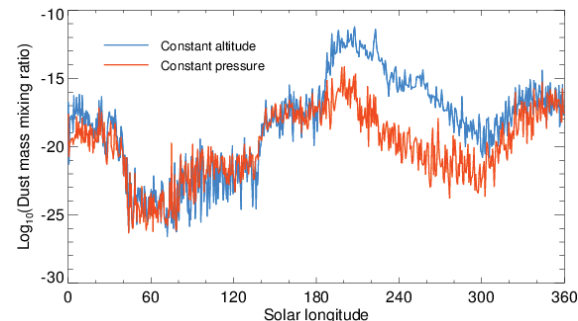


**Figure 5:** Dust mass mixing ratio at the equator and prime meridian at constant altitude (100 km) and pressure (about  $10^{-3}$  Pa).

### Summary:

The main conclusions from this study are:

1. While it seems possible to have dust reaching geometric altitudes (e.g. 90 km) where aerobraking might be performed, in reality dust particles can reach such high altitudes only at the dustiest times of the year when the lower and middle atmospheres tend to be warm and thus expand, meaning that aerobraking would also be performed at higher altitudes at such times. In other words, because aerobraking and dust levitation are controlled by atmospheric density, one should not expect aerobraking spacecraft (assumed to remain at pressure/density levels lower than  $0.01 \text{ Pa}/300 \text{ kg km}^{-3}$ ) to encounter a significant amount of dust particles, which cannot stay airborne at pressures lower than 0.01 Pa for realistic densities and typical sizes.

2. Recent observations (Fedorova et al. 2013) suggest that the Martian atmosphere contains a specific population of very small particles with radii around 0.04–0.07  $\mu\text{m}$ . They are the most likely to reach high altitudes.

3. Detailed 3D Global Circulation Model / Multisize Dust Transport Model numerical simulations have been performed for this study. At times and locations where observations are available (generally between 20–80 km) the model values are broadly in agreement with observations (e.g. McCleese et al. 2010) although some details are not well represented, e.g. thin detached dust layers are not formed using the present convective mixing and thermals parameterizations. This suggests that although a simplified lifting scheme is being used, the model is able to produce a broadly realistic dust distribution.

4. The model is likely to over-predict smaller dust particle sizes in the upper atmosphere, but still there is typically very little dust ( $<10^{-20} \text{ kg/kg}$ ) at pressures lower than about 0.01 Pa or at heights greater than 100 km above the reference areoid.

5. The model shows that large particles ( $>4 \mu\text{m}$ ) are confined to altitudes below around 50 km (even during global dust storms) as a result of the effects of sedimentation. At high altitudes (above 90 km) the effective dust radius is  $<0.2 \mu\text{m}$ , with the larger particles generally corresponding to dust storm periods.

6. The number density of particles above 90 km ranges between  $10^{-2}$ – $1$  particles per  $\text{m}^3$ , a factor of  $10^8$ – $10^{10}$  lower than the near-surface values.

7. Studies such as this with active dust transport will allow us further to refine the dust distribution in prescribed, climate database scenarios and to provide more complete statistics on likely dust behaviour.

**Acknowledgements:** The authors thank ESA for support for this work under contract ESA 4000106548/12/NL/AF.

## References:

- Basu, S., Richardson, M. I., & Wilson, R. J. (2004). Simulation of the Martian dust cycle with the GFDL Mars GCM. *J. Geophys. Res.*, **109**, E11006.
- Basu, S., Wilson, J., Richardson, M., & Ingersoll, A. (2006). Simulation of spontaneous and variable global dust storms with the GFDL Mars GCM. *J. Geophys. Res.*, **111**, E09004.
- Fedorova, A. A., Montmessin, F., Rodin, A. V., Korablev, O. I., A. M., Maltagliati, L., & J-L., Bertaux (2013). Evidence for a bimodal size distribution for the suspended dust particles on mars. *Icarus*, in press.
- Forget, F. (2008a). Martian dust density, particle size and spatial distribution: Part 1) Dust transport model design. Technical report, CNES contract ‘Dust study in the following of MDUST TRP’.
- Forget, F. (2008b). Martian dust density, particle size and spatial distribution: Part 2) Dust size observations and 3D model results. Technical report, CNES contract ‘Dust study in the following of MDUST TRP’.
- Forget, F., Hourdin, F., Fournier, R., Hourdin, C., Talagrand, O., Collins, M., Lewis, S. R., Read, P. L., & Huot, J.-P. (1999). Improved general circulation models of the Martian atmosphere from the surface to above 80 km. *J. Geophys. Res.*, **104**, 24155–24176.
- Kahre, M. A., Hollingsworth, J. L., Haberle, R. M., & Murphy, J. R. (2008). Investigations of the variability of dust particle sizes in the martian atmosphere using the NASA Ames General Circulation Model. *Icarus*, **195**, 576–597.
- Kahre, M. A., Murphy, J. R., & Haberle, R. M. (2006). Modeling the Martian dust cycle and surface dust reservoirs with the NASA Ames general circulation model. *J. Geophys. Res.*, **111**, E06008.
- McCleese, D. J., Heavens, N. G., Schofield, J. T., Abdou, W. A., Bandfield, J. L., Calcutt, S. B., Irwin, P. G. J., Kass, D. M., Kleinböhl, A., Lewis, S. R., Paige, D. A., Read, P. L., Richardson, M. I., Shirley, J. H., Taylor, F. W., Teanby, N., & Zurek, R. W. (2010). Structure and dynamics of the Martian lower and middle atmosphere as observed by the Mars Climate Sounder: Seasonal variations in zonal mean temperature, dust, and water ice aerosols. *J. Geophys. Res.*, **115**, E12016.
- Montabone, L.; Forget, F.; Millour, E. & Lewis, S. R. (2014). Seven-year climatology of dust opacity on Mars. In preparation.
- Mulholland, D. P., Read, P. L., & Lewis, S. R. (2013). Simulating the interannual variability of major dust storms on Mars using variable lifting thresholds. *Icarus*, **223**, 344–358.
- Murphy, J. R., Pollack, J. B., Haberle, R. M., Leovy, C. B., Toon, O. B., & Schaeffer, J. (1995). Three-dimensional numerical simulation of Martian global dust storms. *J. Geophys. Res.*, **100**, 26357–26376.
- Newman, C. E., Lewis, S. R., Read, P. L., & Forget, F. (2002a). Modeling the martian dust cycle, 1. Representations of dust transport processes. *J. Geophys. Res.*, **107**, E05123.
- Newman, C. E., Lewis, S. R., Read, P. L., & Forget, F. (2002b). Modeling the martian dust cycle 2. Multiannual radiatively active dust transport simulations. *J. Geophys. Res.*, **107**, E05124.